Neutron Reflectometry Study of the Segment-Density Profiles in End-Grafted and Irreversibly Adsorbed Layers of Polymer in Good Solvents

C. Marzolin,[†] P. Auroy,[‡] M. Deruelle,[§] J. P. Folkers,[⊥] L. Léger,* and A. Menelle[#]

Laboratoire de Physique de la Matière Condensée, URA CNRS 792, Collège de France, 11 Place Marcelin Berthelot, 75231 Paris Cedex 05, France

Received January 25, 2001; Revised Manuscript Received September 24, 2001

ABSTRACT: The segment density profile of anchored layers of poly(dimethylsiloxane) in good solvents has been measured using neutron reflectometry. Two types of layers have been studied: end-grafted layers (brushes) and irreversibly adsorbed layers, on silicon/silicon dioxide. The latter can be viewed as a polydisperse brush of loops and was obtained by adsorbing the polymer from the melt or from a concentrated solution. A model-free constrained fitting procedure was developed, which gave the concentration profile with a good precision. We present this numerical method and the concentration profiles obtained for the different layers. The profiles of the two types of layers are significantly different. They are in agreement with self-consistent mean field theory for the brushes and with scaling laws descriptions for the irreversibly adsorbed layers. The reflectivity measurement enabled us to verify precisely that the concentration profile in the brush cannot be described by a step function with a Gaussian roughness but has a parabolic shape.

1. Introduction

The properties of anchored polymer layers have been the subject of extensive theoretical and experimental studies in recent years.[1−6] Model systems are obtained when the polymer chains are end-grafted to a nonattractive surface, this layer being called a brush.[7] The case where a polymer melt is put into contact with an adsorbing surface and any segment in the polymer chains can adsorb is more relevant for practical applications, in areas such as adhesion between polymeric materials or control of surface rheology. In some cases, the polymer can adsorb irreversibly and build layers with defined surface excess,[8−10] which remain fixed when the environment of the layer is changed. The behavior of brushes in different environments has been modeled by scaling laws,[7,11−13] self-consistent mean field theory,[4,14−17] and molecular dynamic simulations.[18] The theoretical description of irreversibly adsorbed layers has been made in the scope of scaling laws.[14,19] Previous experimental work has shown that the mean field approach gives a satisfactory description of the segment density profile in brushes swollen by solvents.[13,20−23]

On the other hand, neutron reflectivity has been proved to be a powerful technique to study buried flat interfaces.[24,25] The neutron beam can indeed propagate without much attenuation through many solid substrates like silicon or quartz.[26,27] The structure of polymeric interfaces can be determined with good precision due to the large difference between the scattering lengths of deuterated and hydrogenated polymer species.[28] To get precise information about the concentration profile, care has to be taken in the analysis of the experimental reflectivity. Many numerical methods exist that invert for or adjust the scattering length density profile.[2,23,29,30] Most of these methods are well-suited for multilayers, when the profile has a small number of sharp interfaces. In the case of a smooth variation of the scattering length, however, the reflectivity has no oscillatory feature, and the typical length scales of the profile are not easy to extract.

We present here an investigation through neutron reflectivity of the segment density profiles of two types of surface anchored polymer layers, swollen by a good solvent. The layers are made of poly(dimethylsiloxane) (PDMS) adsorbed or end-grafted on silicon wafers and swollen in toluene or octane at room temperature. A model-free analysis of the reflectivity data has been developed to extract the volume fraction profile in the vicinity of the solid−solution interface. The corresponding profiles are compared to the available theoretical predictions.

2. Experimental Section

Materials. Three kinds of end-functionalized polymers have been used to form the surface-anchored polymer layers. Disilanol-terminated protonated PDMS (hPDMS) were obtained from commercial sources and fractionated to obtain samples with a low polydispersity ($M_w/M_n < 1.1$). *sec*-Butyl-vinyl-terminated hPDMS were prepared by anionic polymerization of hexamethylcyclotrisiloxane (D3)[31] and have a polydispersity index smaller than 1.08. One sample of *sec*-butylsilanol-terminated deuterated PDMS (dPDMS) was prepared by anionic polymerization of perdeuterated D3 and had a molecular weight $M_w = 92$ kg/mol and a polydispersity index of 1.1. These polymers were characterized by gel permeation chromatography and NMR. The substrates were 2 in. diameter ⟨111⟩ silicon wafers that were cleaned before use with methanol and UV/ozone procedure.[32]

[†] Present address: Alcatel Research and Innovation, Route de Nozay, 91461 Marcoussis Cedex, France.
[‡] Present address: Institut Curie, 13 Rue Pierre et Marie Curie, 75231 Paris Cedex 05, France.
[§] Present address: Rhodia Recherche, 69191 Saint Fons, France.
[⊥] Present address: Videojet Systems Intl., 1500 Mittel Bld., Wood Dale, IL 60191.
[#] Laboratoire Léon Brillouin, CEA Saclay, 91191 Gif sur Yvette Cedex, France.
* Corresponding author.

10.1021/ma010156z CCC: $20.00
Published on Web 11/08/2001

Preparation of the Samples. The formation of the end-grafted layers required two steps.[33] First, a dense thin layer of Si−H functionalized PDMS oligomers was self-assembled on the silicon wafer surface. The thickness of this sublayer was checked to be 1.7−1.8 nm by X-ray reflectometry, and its role was to prevent any further adsorption of the end-grafted chains on the substrate. The second step consisted of end-grafting long PDMS chains on the Si−H layer by a hydrosilylation reaction catalyzed by Karstedt platinum. Both vinyl- and silanol-terminated PDMS could graft in this way, the grafting kinetics being much faster for the vinyl than for the silanol end group. The polymer concentration in the reaction bath allowed one to control the surface density of grafted chains. Both the polymerization index, N, and the surface density, Σ, of the grafted chains could thus be chosen independently.[34]

To obtain irreversibly adsorbed PDMS layers, the bare clean wafers were incubated with a PDMS melt or concentrated solutions for 12−24 h at 110 °C. Unattached polymer chains were then rinsed away by dipping the wafers in toluene for several hours. The quantity of polymer remaining on the surface after drying under nitrogen was determined by X-ray reflectivity. Indeed, the thickness of the dry layer, h_0, the polymerization index of the surface anchored chains, N, and the surface density, Σ, are related through $h_0 = aN\Sigma$ (a is the size of a monomer), and h_0 is a measure of the surface excess.[34]

Neutron Reflectivity. The experiments were performed on the time-of-flight spectrometer EROS at LLB* in "Commissariat à l'Energie Atomique" in Saclay. The angle of incidence of the beam was 0.8°. The analysis of the reflectivity data was made with a constrained least-squares algorithm to adjust the scattering length density profiles. The reflectivity was computed with the matrix method and corrected for resolution effects. The scattering length density profile was sampled into a 30-box profile. Let us call ϕ_i the volume fraction of polymer in the box i of width d_i, $i = 1...\nu$. The scattering length density in the box i is then $Nb_0 + \phi_i(Nb_1 - Nb_0)$, where Nb_0 and Nb_1 are respectively the scattering length density of the solvent and of the polymer. The function to minimize in the fit is $\chi'^2 = \chi^2 + \mu\beta$ where $\chi^2 = [1/(M - \nu)]\sum_i^M(\log R_i - \log R(k_i))^2(R_i^2/\sigma_i^2)$ is the usual mean-square residual function. M is the number of data points, R_i is the experimental reflectivity for the momentum transfer k_i with an error σ_i, R is the simulated reflectivity, and β is a penalty parameter defined by $\beta = \sum_i(\phi_{i+1} - \phi_i)^2$. The number of degrees of freedom is ν because the width of the boxes is kept constant. This choice of boxes having a constant width does not restrict the generality of the procedure as neutrons, like waves, are sensitive to the product of the width by the scattering length density. The constraint μ allows introducing an "elasticity" in the concentration profile. This term is similar to the entropic term in the maximum entropy method[22] and can be viewed as an elastic energy of the concentration profile. The introduction of this constraint, very similar to that proposed by Pedersen,[35] was motivated by the fact that the effective number of degrees of freedom was much too large for the fit to be stable. Furthermore, running a fit with no constraint always reached a nonphysical "saw-tooth" profile, which was highly dependent on the initial starting parameters. The constraint allowed reducing the number of degrees of freedom by coupling the different sublayers. The choice of the constraint was however crucial and was made in the following way.[35,36] The variation of χ^2 as a function of μ when χ'^2 is minimum is first a very slowly increasing function when starting from $\mu = 0$. Above a critical value, μ_c, the variation becomes faster than exponential. This value μ_c can be chosen to define the "best" fit. It corresponds to the smoothest profile giving a satisfactory fit of the experimental reflectivity. Practically, the fit was started with a flat profile as initial condition and with a large μ value. This value was then gradually decreased until the iteration seemed to reach a minimum of χ^2. The value of μ was then kept constant, so that the contributions of the "elastic" term and of the error term in χ'^2 were of the same order. The whole fitting procedure could be implemented on a 400 MHz PC.

Table 1. Characteristics of the PDMS Layers Used in This Study[a]

layer	mN (kg/mol)	h_0 (Å)	solvent	χ^2
adsorbed (d)	92	110	octane	1.0
grafted (d)	92	67	octane	0.9
adsorbed (h)	18	70	toluene	10
adsorbed (h)	62	134	toluene	3.2
adsorbed (h)	160	186	toluene	3.5
adsorbed (h)	450	240	toluene	0.9
grafted (h)	17	75	toluene	1.4
grafted (h)	60	195	toluene	1.0
grafted (h)	80	201	toluene	1.1

[a] (h) stands for hydrogenated PDMS and (d) for deuterated. N is the polymerization index of the chains related to the weight-average molecular weight by $M_W = mN$, with m the molar mass of the monomer, $m = 74$ g/mol. h_0 is the thickness of the dry layer.

Another important control is the knowledge of the surface excess. We knew indeed the quantity of polymer attached to the surface, given experimentally by the thickness of the dry layer, h_0. Thus, calculating $\int_0^\infty\phi(z)\,dz$ with the best fitted profile enabled us to control that this best fit was physically acceptable.

Finally, the thickness of the native oxide layer and, if needed, of the primer layer were allowed to vary within 0.2 nm from their experimental value measured independently by ellipsometry or X-ray reflectivity.

3. Results

Despite the above-described controls on the fitting procedure, the uniqueness of the concentration profile thus determined was not guaranteed. We noticed however that whatever the starting value of the fit was, all the profiles found having a surface excess compatible with the measured value did not differ by more than 5% from one another. This pseudo-uniqueness was satisfactory insofar as the reflectivity curves did not seem to carry as much information in our case as what can be observed for hard multilayers, that is, well-defined oscillations. Table 1 displays the parameters of the samples and the mean-square residuals. Figures 1a−4a show the normalized neutron reflectivity R/R_F as a function of the momentum transfer k, where R_F is the Fresnel reflectivity, for the different layers investigated. The scattering length density of the silicon and that of the solvent were determined experimentally and used as boundary conditions for the fit and for the calculation of R_F. The corresponding concentration profiles determined by the fit are shown in Figures 1b−4b.

As can be seen in the figures, the presence of the polymer, even in small quantities, has a drastic effect on the reflectivity. All the reflectivity curves exhibit oscillatory features, which are characteristic of the finite length of the swollen layer and follow well the experimental data. The concentration profiles found for brushes and adsorbed layers have significantly different shapes. They differ mainly by the polymer volume fraction in the vicinity of the solid surface. The volume fraction in adsorbed layers reaches values up to 90% with a very fast variation close to the substrate (Figures 1b and 2b). The volume fraction in brushes, however, remains between 10 and 50% and roughly constant close to the surface (Figures 3b and 4b). This qualitative difference shows that there was much less adsorption on the surface (bare silica in the case of adsorbed layers, SiH sublayer in the case of grafted layers) in the case of a brush than in that of an adsorbed layer.

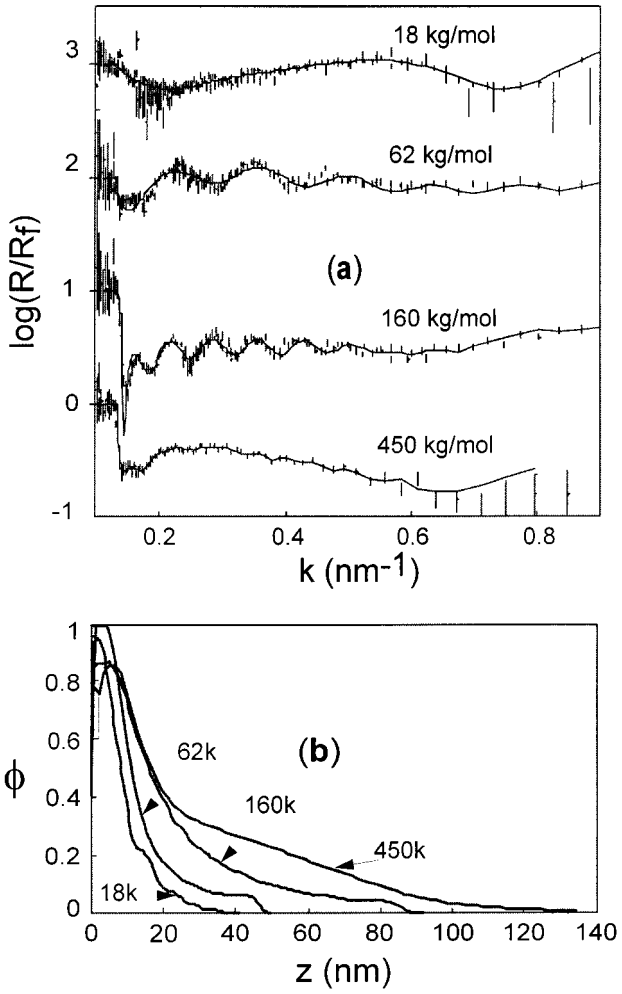

Figure 1. (a) Experimental (symbols) and fitted (lines) normalized reflectivity curves for irreversibly adsorbed layers of hPDMS having different weight-average molecular weights, swollen in deuterated toluene. For clarity, the curves have been displaced vertically by 1 decade with respect to each other. (b) Volume fraction profiles corresponding to the fits.

Table 2. Excluded-Volume Parameter Used in the Comparison of the Experimental Profiles and the Theoretical Parabolic Profile for the Grafted Layers

mN (kg/mol)	v
17	0.68
60	0.57
80	0.49
92 (deuterated)	0.88

4. Discussion

Grafted Layers. The behavior of end-tethered polymer layers in good solvents was first modeled by Alexander and de Gennes in a scaling approach.[1] Assuming that all the grafted chains swell the same way, they found the concentration profile to be a step function, the local internal structure of the brush being that of a semidilute solution. The use of self-consistent mean field theory enabled other authors[4,16,37] to take into account the connectivity of the chain and to derive the so-called parabolic profile, compatible with some experimental observations.[20,38] The volume fraction is given by $\phi(z) = \phi_0(1 - z^2/H^2)$ with $H = vacN\Sigma^{1/3}$ and $\phi_0 = (3\pi^2/8)a^{-2}N^{-2}H^2$, where N is the polymerization index of the chains, Σ their grafting density, a the monomer size, v is the excluded-volume parameter, and c is a constant ($c = 0.74$). The grafting density in our layers is determined by the dry thickness of the layer, $h_0 = aN\Sigma$.

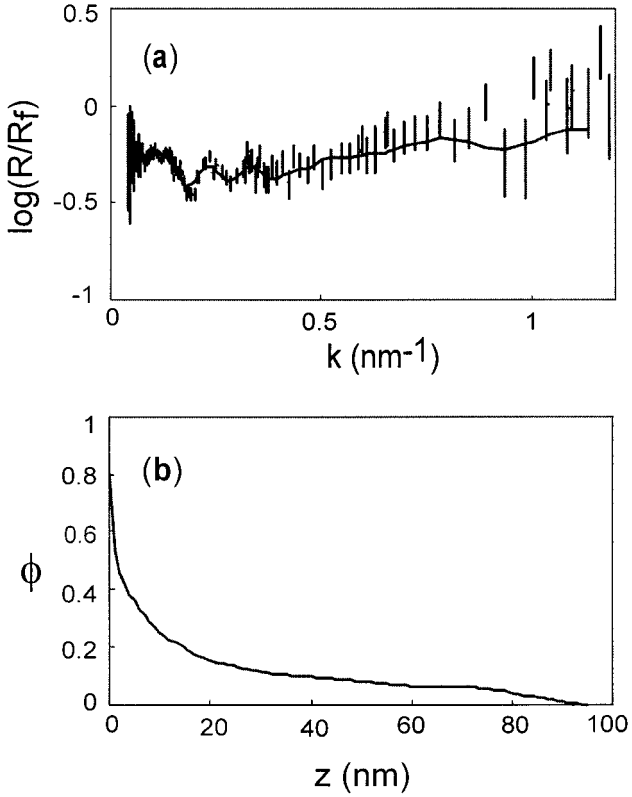

Figure 2. (a) Experimental (symbols) and fitted (line) normalized reflectivity curves for an irreversibly adsorbed layer of dPDMS (M_W = 92 kg/mol) swollen in octane. (b) Volume fraction profile corresponding to the fit.

The reflectivity data could not be correctly fitted with a simple step function plus a Gaussian roughness. The corresponding fits gave χ^2 ranging from 20 to 100. This shows that the step function profile is not sufficient to describe the inner structure of the brush. A model-dependent fit with a two-parameter (H and ϕ_0) parabolic profile gave unsatisfactory χ^2 in the range 15−30. We thus compared the parabolic profile to the free-form fitted profiles by adjusting manually the excluded-volume parameter v. The corresponding adjusted values are displayed in Table 2 and show only a slight dependence on N for a given solvent. The observed difference in v between the deuterated and the protonated brush can come from isotopic differences or solvent quality differences between octane and toluene. Some data exist in the literature on the differences in surface energy between deuterated and protonated polymers,[39] and the value for polystyrene is very small (0.1 mJ/m^2). We thus expect the relative difference in the interaction parameter to be very small and not responsible for the observed difference between the adjusted v values. We rather think that this is indicative of the fact that octane is a better solvent of PDMS than toluene.

The shapes of the experimental profiles are in good qualitative agreement with the predicted ones (Figures 5 and 6). A few differences can however be noticed. The tail of the experimental profile is smoother, and a maximum in the concentration exists close to the wall. This smooth tail of the profile can be explained by the polydispersity of the grafted chains or by a minute

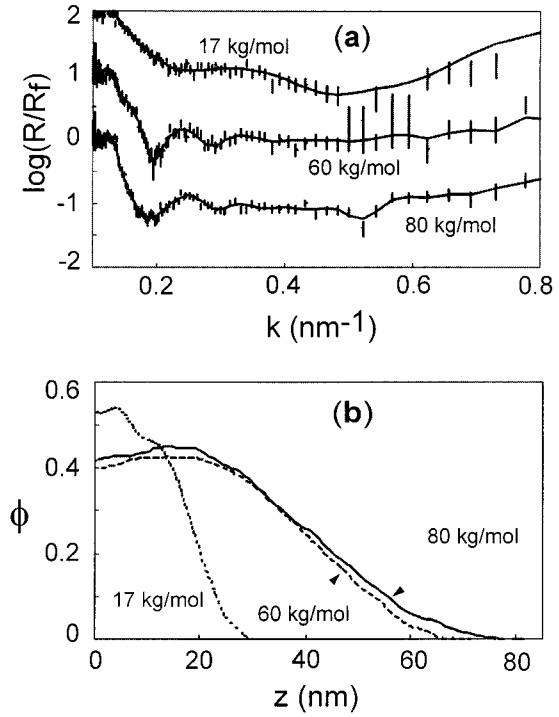

Figure 3. (a) Experimental (symbols) and fitted (lines) normalized reflectivity curves for grafted layers of hPDMS having different molecular weights, swollen in deuterated toluene. For clarity, the curves have been displaced vertically by 1 decade with respect to each other. (b) Volume fraction profile corresponding to the fits.

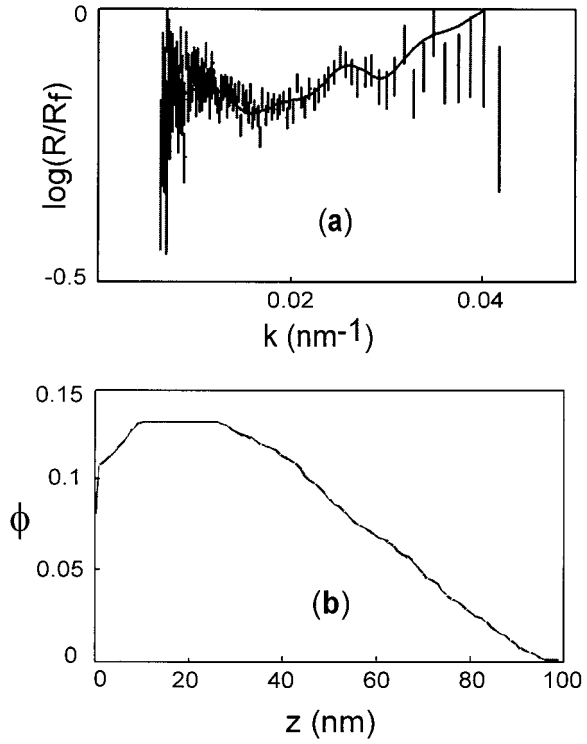

Figure 4. (a) Experimental (symbols) and fitted (line) normalized reflectivity curves for a grafted layer of dPDMS (M_W = 92 kg/mol) swollen in octane. (b) Volume fraction profile corresponding to the fit.

amount of adsorption on the surface. The slight depletion in the vicinity of the interface is due to the fact that the surface, protected by the SiH layer is essentially repulsive for the polymer. Scaling theories

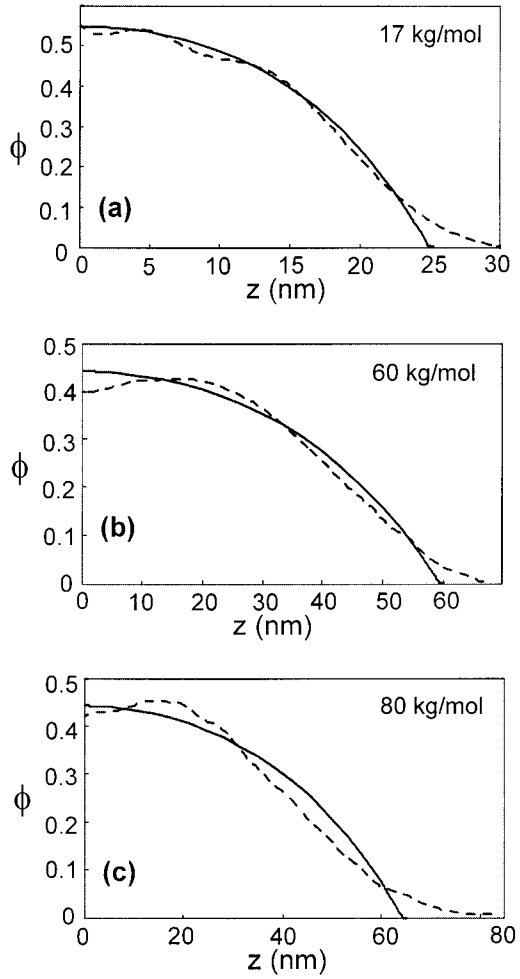

Figure 5. Comparison between the experimental volume fraction profiles (– –) and the theoretical parabolic profiles (—) corresponding to the experimentally measured surface excess for the grafted layers of hPDMS swollen in deuterated toluene.

predict a depletion thickness D, with $D = a\Sigma^{-1/2}$ the distance between grafting points. The samples have a grafting distance $D = 2$ nm for the protonated layers and $D = 4.5$ nm for the deuterated one. The data show a depletion of ca. 8 nm, larger than expected. This discrepancy seems significant and might be a small artifact of the fitting method, similar to that observed with the Max Ent method.[40]

Irreversibly Adsorbed Layers. Irreversibly adsorbed polymer layers have been modeled in the framework of scaling descriptions.[19,41,42] The inner structure of the layer is very different from that of a grafted layer because each chain has many contact points with the surface as shown schematically in Figure 7. This affects the concentration profile in the swollen layer. Scaling arguments lead to a volume fraction following the scaling law $\phi(z) \propto z^{-2/5}$. The experimental data, however, could not be fitted using this type of profile, mainly because this scaling law gives a nonphysical step at the end of the layer. This step, which is suppressed when the molecular weight becomes infinite, can also be removed by an exact calculation of the monomer concentration following Guiselin's approach as developed below.

As in ref 19, the following assumptions are needed in order to model the layer: (i) An attractive wall is put into contact with a concentrated solution or a melt of

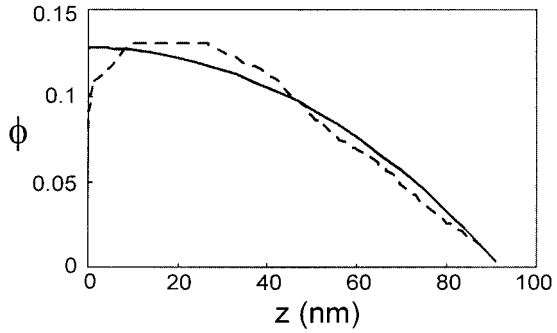

Figure 6. Comparison between the experimental volume fraction profile (– –) in a grafted layer of dPDMS (92 kg/mol) swollen in octane and the parabolic profile (—) corresponding to the experimental surface excess.

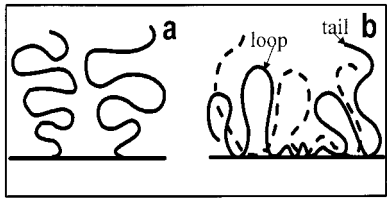

Figure 7. Schematic representation of (a) a grafted layer and (b) an irreversibly adsorbed layer. The adsorbed layer displays a number of loops (sequence of adjacent monomers not attached to the wall except at the two extremities of the corresponding subchain) and a few tails (subchain with only one extremity attached to the wall). On the contrary, the grafted layer only contains tails. In the adsorbed layer, trains can also be formed, i.e., sequence of adjacent monomers all attached to the surface.

polymer chains and the adsorption sites saturates rapidly. (ii) The unadsorbed polymer is rinsed away with a good solvent. (iii) The swollen layer can be described by the use of a loop distribution only, this distribution remaining constant with time. Each loop made of $2n$ monomers swells like two end-grafted chains of size n. (iv) The local structure of the layer is that of an Alexander–de Gennes brush whose grafting density depends on the distance to the wall.

The description in terms of loops, trains, and tails can be found in refs 41 and 43. We assume that the trains can be described as loops of size 1. Once the layer has been formed, the loop and tail distributions are defined. Following Guiselin's approach, we call $D'_1(n)$ and $D'_2(n)$ the number per area a^2 of loops and tails made of n monomers, respectively. Then the number per area a^2 of pseudotails made of more than n monomers is

$$D(n) = \int_n^N (2D_1'(2n) + D_2'(n))\,\mathrm{d}n$$

Assuming that the pseudotails are all stretched the same way, we can call $z(n)$ the distance from the surface of the nth monomer of the pseudotails made of more than n monomers. Then z is an increasing function of n. At a distance $z(n)$ from the surface, the local structure of the layer is that of a brush with a grafting density $\mathscr{D}(n)$. Thus, we have

$$\frac{\mathrm{d}z}{\mathrm{d}n} = a\mathscr{D}(n)^{1/3}$$

$$\phi(z) = \mathscr{D}(n)^{2/3} \qquad (1)$$

provided that $\mathscr{D}(n)$ is larger than the overlapping density $N^{-5/6}$. If $\mathscr{D}(n)$ is smaller, the layer is not stretched and remains in the mushroom regime.

Adsorption from a Melt. We consider the case where the adsorption site density is high. The adsorption from the melt gives a surface excess of $a^{-2}N^{-1/2}$. Guiselin showed that the loop distribution $f_1(n)$, which is the number per chains of loops of size n, is proportional to $n^{-3/2}$ or more precisely $f_1(n) = {}^1/_2 N^{1/2} n^{-3/2}$.

Now the tail distribution $f_2(n)$ can be derived the same way. Let us assume that there is on average only one tail per chain. This can be the case if we allow one end of the chain to graft chemically to the surface. As the average number of contact points to the surface is $N^{1/2}$, the average length of the tail is $N^{1/2}$. Then $f_2(n)$ is a solution of

$$\int_1^N f_2(n)\,\mathrm{d}n = 1$$

$$\int_1^N n f_2(n)\,\mathrm{d}n = N^{1/2}$$

If we assume that $f_2(n)$ follows a power law, we find $f_2(n) = n^{-3/2}/2$. Then

$$\mathscr{D}(n) = N^{-1/2}\left(2\int_{2n}^N f_1(n)\,\mathrm{d}n + \int_n^N f_2(n)\,\mathrm{d}n\right) \quad \text{for } n \le N/2$$

and

$$\mathscr{D}(n) = N^{-1/2}\int_n^N f_2(n)\,\mathrm{d}n \quad \text{for } n > N/2$$

The concentration profile is found by solving eqs 1, which are valid as long as the pseudotails are stretched. The density of pseudotails with a size larger than $N/2$ is $\mathscr{D}(N/2) = (\sqrt{2} - 1)N^{-1}$, of the order of the critical overlapping density $2^{6/5}N^{-6/5}$ for achievable molecular weights. This means that the tails are not stretched and do not increase significantly the thickness of the layer. This situation is quite different from what is observed in a reversibly adsorbed layer, whose structure is mostly determined by the tails.[44,45] We will thus neglect the presence of the tails in the irreversibly adsorbed layer by neglecting $f_2(n)$, which leads to

$$\mathscr{D}(n) = 2((2n)^{-1/2} - N^{-1/2}), \quad n \le N/2 \qquad (2)$$

The pseudobrush can thus be well described as a polydisperse brush of loops.

Concentration Profile in a Solvent. The relations that give the concentration profile come from eqs 1 and 2:

$$z(n) = 2^{1/3}a\int_1^n ((2n')^{-1/2} - N^{-1/2})^{1/3}\,\mathrm{d}n'$$

$$\phi(z(n)) = 2^{2/3}((2n)^{-1/2} - N^{-1/2})^{2/3} \qquad (3)$$

The integration can be conducted analytically but gives no useful expression. The thickness of the layer and the concentration profile were determined *numerically* using Mathematica. We found that the total thickness of the layer can be written $z(N/2) = aN^{5/6}c(N)$ where $c(N)$ is a function varying slowly from 0.4 to 0.5 as N goes from 100 to infinity. The scaling law $aN^{5/6}$ is thus a good approximation of this expression for large N. As a comparison, an Alexander–de Gennes brush made of monodisperse loops, which can be obtained by grafting both ends of the chains, would have a thickness of the same form with $c = 0.63$ (given by doubling the

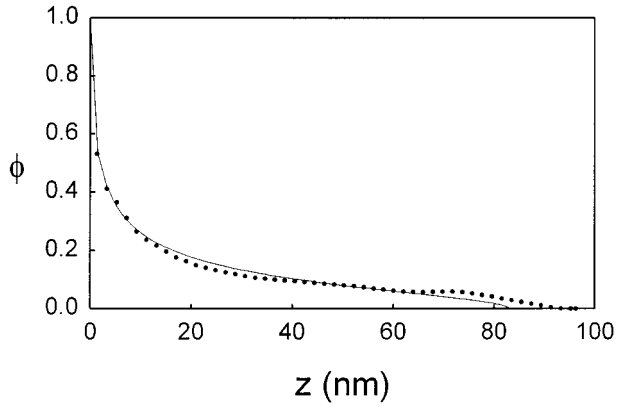

Figure 8. Comparison between the theoretical profile inside an irreversibly adsorbed layer according to the scaling law analysis developed in the present paper (numerical resolution of eq 3) (line) and the experimental one (dots) for an adsorbed layer of dPDMS (92 kg/mol, $a = 0.48$ nm) in a good solvent.

grafting density and dividing the molecular weight by 2). The total thickness of the swollen pseudo-brush is slightly smaller than that of a brush of monodisperse loops.

The concentration profile close to the wall has the form predicted by Guiselin $\phi(z) \propto z^{-2/5}$, which can be obtained by neglecting $N^{-1/2}$in eqs 3. This power law, however, cannot describe the outer part of the layer, since the concentration goes continuously to 0.

Figure 8 shows a comparison between the experimental profile and the numerically computed one (from eq 3) for the dPDMS layer in octane. As predicted, the volume fraction close to the attractive surface is high and decreases rapidly. The profile shows a long tail where the concentration is roughly 10%, induced by the presence of large loops. The agreement with the model is good in that case (deuterated PDMS in octane). This is however not the case for the hydrogenated layers in deuterated toluene, which appear less swollen than expected. This effect is similar to that observed for the brushes and might be due to a better quality of octane compared to toluene. A preferential interaction between the surface and the hydrogenated PDMS compared to the deuterated species could lead to similar observations. We however expect isotopic-selective adsorption effects to be stronger in this case of adsorbed layers, and additional experiments would be necessary to differentiate the two effects.

5. Conclusions

Two different types of poly(dimethylsiloxane) layers attached to a flat surface have been generated: irreversibly adsorbed layers and end-grafted layers. We have used neutron reflectivity to determine the volume fraction profile inside those polymer layers when swollen with a good solvent. The reflectivity data have been adjusted with a model-free constrained fitting procedure. With this method the volume fraction could be determined with good accuracy and compared with the different available theoretical models.

In the case of the end-grafted layers the volume fraction profile was compared to scaling law predictions and with self-consistent mean field models. The parabolic profile derived from the mean field theory could describe the main shape of the experimental profile. A minute discrepancy was found in the tail of the profile and could be explained by the polydispersity of the chains. A weak depletion in the vicinity of the surface was also observed and attributed to a short-range repulsion of the surface. The adjustment of the excluded volume parameter v was possible, and the value found for deuterated PDMS in octane was $v = 0.88$ whereas the value found for hydrogenated PMDS in toluene was between 0.49 and 0.68.

In the case of irreversibly adsorbed layers, a scaling law approach, based on Guiselin's ideas, was developed to take into account the finite length of the chains. This approach gave a good description of the main features of the concentration profiles. The fast decay of the concentration from the surface and the long tail of the profile were qualitatively in good agreement with this prediction.

Acknowledgment. This work was supported by Saint-Gobain Recherche and Rhône-Poulenc.

References and Notes

(1) Alexander, S. *J. Phys.* (*Paris*) **1977**, *38*, 977−981.
(2) Auroy, P.; Auvray, L.; Léger, L. *Macromolecules* **1991**, *24*, 5158−5166.
(3) Cohen-Addad, J. P. *Polymer* **1989**, *30*, 1821−1823.
(4) Zhulina, E. B.; Borisov, O. V.; Brombacher, L. *Macromolecules* **1991**, *24*, 4679−4690.
(5) Shull, K. R. *J. Chem. Phys.* **1991**, *94*, 5723−5728.
(6) Lee, L. T.; Kent, M. S. *Phys. Rev. Lett.* **1997**, *79*, 2899−2902.
(7) de Gennes, P. G. *Macromolecules* **1980**, *13*, 1069−1075.
(8) Marques, C.; Joanny, J. F. *J. Phys. (Paris)* **1988**, *49*, 1103−1109.
(9) Auvray, L.; Auroy, P.; Cruz, M. *J. Phys. I* **1992**, *2*, 943−954.
(10) Auvray, L.; Cruz, M.; Auroy, P. *J. Phys. II* **1992**, *2*, 1133−1140.
(11) Ferreira, P. G.; Ajdari, A.; Leibler, L. *Macromolecules* **1998**, *31*, 3994−4003.
(12) Aubouy, M.; Raphaël, E. *C. R. Acad. Sci. Paris II* **1994**, *318* (9), 1181−1184.
(13) Auroy, P.; Mir, Y.; Auvray, L. *Phys. Rev. Lett.* **1992**, *69* (1), 93−95.
(14) Auroy, P.; Auvray, L.; Léger, L. *Macromolecules* **1991**, *24*, 2523−2528.
(15) Johner, A.; Bonet-Avalos, J.; van der Linden, C. C.; Semenov, A. N.; Joanny, J. F. *Macromolecules* **1996**, *29*, 3629−3638.
(16) Shull, K. R. *Macromolecules* **1996**, *29*, 2659−2666.
(17) Baranowski, R.; Whitmore, M. D. *J. Chem. Phys.* **1998**, *108*, 9885−9892.
(18) Grest, G. S. *J. Chem Phys.* **1996**, *105*, 5532−5541.
(19) Guiselin, O. *Europhys. Lett.* **1992**, *17*, 225−230.
(20) Jones, R. A. L.; Norton, L. J.; Shull, K. R.; Kramer, E. J.; Felcher, G. P.; Karim, A.; Fetters, L. J. *Macromolecules* **1992**, *25*, 2359−2368.
(21) Karim, A.; Satija, S. K.; Douglas, J. F.; Ankner, J. F.; Fetters, L. J. *Phys. Rev. Lett.* **1994**, *73*, 3407−3410.
(22) Sivia, D. S.; Hamilton, W. A.; Smith, G. S. *Physica B* **1991**, *173*, 121−138.
(23) Kent, M. S.; Factor, B. J.; Satija, S.; Gallagher, P.; Smith, G. S. *Macromolecules* **1996**, *29*, 2843−2849.
(24) Clarke, C. J.; et al. *Macromolecules* **1995**, *28*, 2042−2049.
(25) Geoghegan, M.; Clarke, C. J.; Boué, F.; Menelle, A.; Russ, T.; Bucknall, D. G. *Macromolecules* **1999**, *32*, 5106−5114.
(26) Hayter, J. B.; Highfield, R. R.; Pullman, B. J.; Thomas, R. K.; McMullen, A. I.; Penfold, J. *J. Chem. Soc., Faraday Trans.* **1981**, *77*, 1437−1448.
(27) Viallat, A.; Cohen-Addad, J. P.; Pouchelon, A. *Polymer* **1986**, *27*, 843−848.
(28) Geoghegan, M.; et al. *Eur. Phys. J. B* **1998**, *3*, 83−96.
(29) Kunz, K.; Reiter, J.; Götzelmann, A.; Stamm, M. *Macromolecules* **1993**, *26*, 4316−4323.
(30) Politsch, E.; Cevc, G.; Wurlitzer, A.; Lösche, M. *Macromolecules* **2001**, *34*, 1328−1333.
(31) Oulad Hammouch, S.; Beinert, G. J.; Zilliox, J. G.; Herz, J. E. *Polymer* **1995**, *36*, 421−426.
(32) Vig, J. R. In *Treatise on Clean Surfaces Technology;* Mittal, K. L., Ed.; Plenum Press: New York, 1987.
(33) Folkers, J. P.; Léger, L.; Deruelle, M., submitted to *Langmuir*.
(34) Léger, L.; Raphaël, E.; Hervet, H. *Adv. Polym. Sci.* **1999**, *138*, 185−225.

(35) Pedersen, J. S.; Hamley, I. W. *Physica B* **1994**, *198*, 16−23.
(36) Pedersen, J. *J. Appl. Crystallogr.* **1992**, *25*, 129−145.
(37) Milner, S. T. *Macromolecules* **1988**, *21*, 2610−2619.
(38) Mansfield, T. L.; et al. *Macromolecules* **1995**, *28*, 492−499.
(39) Jones, R. A. L.; et al. *Phys. Rev. Lett.* **1989**, *62*, 280−283.
(40) Geoghegan, M.; et al. *Phys. Rev. E* **1996**, *53*, 825−837.
(41) Ausseré, D. *J. Phys. (Paris)* **1989**, *50*, 3021−3042.
(42) Ji, H.; et al. *Macromolecules* **1990**, *23*, 698−707.
(43) Scheutjens, J. M. H. M.; Fleer, G. J. *J. Phys. Chem.* **1980**, *84*, 178−190.
(44) Semenov, A. N.; Joanny, J.-F. *Europhys. Lett.* **1995**, *29*, 279−284.
(45) Semenov, A. N.; Bonet-Avalos, J.; Johner, A.; Joanny, J. F. *Macromolecules* **1996**, *29*, 2179−2196.

MA010156Z